Electrochemical Formation of p-Type $Bi_{0.5}Sb_{1.5}Te_3$ Thick Films onto Nickel

C. Lei, M. Burton, and Iris S. Nandhakumar[z]

School of Chemistry, University of Southampton, Southampton SO17 1BJ, United Kigdom

Bismuth-telluride-based alloys are currently the best commercially available thermoelectric materials for applications at room temperatures. Up to 150 micron thick layers of bismuth antimony telluride ($Bi_{0.5}Sb_{1.5}Te_3$) were directly deposited onto nickel by either potenstiostatic or potentiodynamic electrodeposition. Cyclic voltammetry was employed to identify the optimal deposition potential. The films were characterized by scanning electron microscopy, energy dispersive X-rays and X-ray diffraction. The p-type films were found to be well adherent, uniform and stoichiometric with a high power factor of 2.3×10^{-4} W m^{-1} K^{-2} at film growth rates of up to 40 μm h^{-1}.

Manuscript submitted December 15, 2016; revised manuscript received February 6, 2017. Published February 14, 2017.

Power harvesting from thermoelectric (TE) devices is seen as a highly promising route toward sustainable energy, as electricity can be generated from waste heat using the Seebeck effect.[1,2] This however is contingent on fabricating materials with higher thermoelectric efficiencies than currently available. Bismuth-telluride-based alloys are currently the best commercially available thermoelectric materials for applications at room temperatures.[3]

Whilst a wide range of fabrication techniques[4,5] exists for the production of bismuth telluride compounds, including molecular organic vapor phase deposition (MOVPD), molecular beam epitaxy (MBE), liquid phase epitaxy (LPE) and bulk powder synthesis, these methods have proven to be quite costly and/or difficult to realize. Electrochemical deposition on the other hand provides an attractive low-cost, room temperature and scalable route and bismuth telluride alloys prepared in this way are a striking example of the type of high-quality thermoelectric materials that can be prepared in this way.[6]

Whilst there have been many reports on the electrochemical deposition of n-type Bi_2Te_3,[7,8] the preparation of p-type bismuth antimony telluride ($Bi_{0.5}Sb_{1.5}Te_3$)[10–12] has received very little attention with film thicknesses not exceeding 20 microns. The realization of functional TE devices for commercial applications however relies on incorporating the materials as both n and p-type thick films, e.g. such as those encountered in vertical TE designs on vehicle exhaust pipes.[8,13,14] The main challenge with the electrodeposition of p-type $Bi_{0.5}Sb_{1.5}Te_3$ has been attributed to the low solubility of antimony in aqueous electrolytes which results in insufficient amounts of Sb^{3+}. This makes the preparation of thick layers of $Bi_{0.5}Sb_{1.5}Te_3$ extremely challenging as it requires fast deposition rates (∼10 μm/hour) to make the process commercially viable and hence necessitates high concentrations of the respective precursors in the electrolyte. In addition commercial TE devices require the use of a nickel diffusion barrier to prevent diffusion of tin from the solder and copper from the electrodes into the p- and n-type TE legs. To the best of our knowledge there are no literature studies that have reported the electrochemical depositon of $Bi_{0.5}Sb_{1.5}Te_3$ onto nickel (Ni) at the achieved thicknesses of 150 microns with a high power factor of 2.3×10^{-4} W m^{-1} K^{-2}.

The work presented here reports the reproducible electrochemical fabrication of up to 150 micron thick layers of uniform and stoichiometric layers of p-type $Bi_{0.5}Sb_{1.5}Te_3$ onto Ni with a high power factor of 2.3×10^{-4} W m^{-1} K^{-2} at fast film growth rates of 40 μm/hr in the case of potentiodynamic deposition which are suitable for incorporation into commercial TE devices targeted at room temperature operations. Potentiostatic and potentiodynamic electrodeposition of the $Bi_{0.5}Sb_{1.5}Te_3$ films has been investigated.

[z]E-mail: iris@soton.ac.uk

Experimental

Film fabrication.—Electrolytes were composed of 5 mM Ammonium bismuth citrate ($Bi(NH_4)_3Cit$, Sigma-Aldrich, ≥99.0%), 20 mM potassium antimonyl tartrate trihydrate (K_2Sb_2Tar, Sigma-Aldrich, ≥99.0%), 30 mM tellurium dioxide (TeO_2, Alfa Aesar, 99.99%),) in 1 M nitric acid (HNO_3, Fisher 70%) with 100 to 300 mM sodium citrate (Na_3Cit, Sigma-Aldrich ≥99.0%). Ethylenediaminetetraacetic acid disodium (Na-EDTA, Sigma-Aldrich, ≥99.0%) was added at concentrations of 5 to 30 mM. Water from a Purite Select Fusion 160 (Ondeo) water purification system (resistivity 18.2 MΩ cm) was used to prepare all electrolyte solutions. To complex Te^{2+} TeO_2 powder is first dissolved in a small volume of concentrated NaOH solution, and then neutralized with citric acid (H_3Cit, Sigma-Aldrich, 99 + %).

A conventional three-electrode electrochemical cell connected to an Ivium Technology potentiostat/galvanostat was used for performing all electrochemical deposition experiments with a large-area platinum grid counter electrode and a Saturated calomel electrode (SCE) reference electrode. A 1 cm^2 Ni foil (Alfa Aesar, 0.127 mm thick, 99 + %) served as the working electrode. This was etched in concentrated HCl for 1 min, followed by etching in 1 M HNO_3 solution at a potential of +0.15 V vs SCE for 30 seconds to remove any surface oxide to enable better adhesion of the Bi-Te-Sb deposits to the Ni surface. The Ni working electrodes were then thoroughly rinsed in deionized water. Electrodeposition was carried out by potentiostatic as well as potentiodynamic (pulsed) deposition. Potentiostatic electrodeposition was perfomed at potentials of −0.22 V, −0.25 V, −0.28 V, −0.31 V, −0.35 V vs SCE. The potentiodynamic (pulsed) electrodeposition employed zero current resting pulses for 4s, followed by deposition pulses of 10 ms at either −0.20 V or −0.25 V vs. SCE.

Characterization.—The electrodeposited Bi-Te-Sb films were imaged by scanning electron microscope (SEM, JSM 5910) equipped with Energy dispersive X-ray (EDX, Oxford Inca 300) for compositional analysis.

The Seebeck coefficient, S, was measured with a custom-built measurement unit that was calibrated against a polycrystalline bismuth foil reference standard with an accuracy of 5%. A commercial Hall effect measurement unit (HMS 300 from Ecopia) was employed for determining the Hall mobility, electrical conductivity and carrier concentration of the deposited films in-plane by the van der Pauw technique (direct current (dc) of 19 mA and a permanent magnetic field of 0.37 T at room temperature). All electrodeposited films were delaminated from the underlying Ni substrate prior to Hall effect measurements by embedding them in an epoxy layer to ascertain that there was no interference from the Ni substrate.

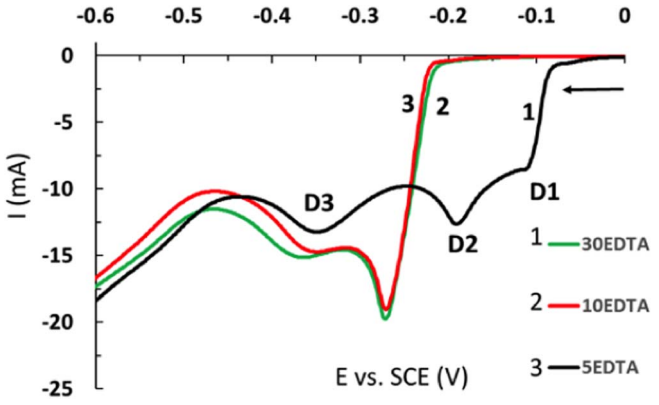

Figure 1. Cyclic voltammograms recorded at a 1 cm^2 Ni working electrode vs. SCE immersed in electrolyte solutions of 5 mM $Bi(NH_4)_3Cit$, 20 mM K_2Sb_2Tar, 30 mM TeO_2, 200 mM Na_3Cit in 1 M HNO_3 with Na-EDTA concentrations of 5 mM, 10 mM and 30 mM. The CVs were obtained at room temperature at a scan rate of 20 mV/s.

Results and Discussion

Cyclic voltammetry (CV) was employed to identify the optimum deposition potential for the formation of stoichiometric layers of $Bi_{0.5}Sb_{1.5}Te_3$ on Ni. Figure 1 shows representative cyclic voltammograms recorded at a 1 cm^2 Ni working electrode immersed in electrolytes containing 5 mM $Bi(NH_4)_3Cit$, 20 mM K_2Sb_2Tar, 30 mM TeO_2, 200 mM Na_3Cit in 1 M HNO_3. Na-EDTA at concentrations of 5 mM, 10 mM and 30 mM was added to the electrolyte as well. The Ni working electrode potential was scanned from +0.0 V to −0.6 V vs. SCE. At small concentrations of Na-EDTA, three reduction peaks can be identified (cf. Fig. 1) which have been labeled as D1-D3. Peak D1 corresponds to bismuth (Bi) deposition, D2 to tellurium (Te) deposition, and D3 to antimony (Sb) deposition. As the concentration of Na-EDTA is increased to 10 mM and above, the D1 and D2 reduction peaks combine to form one reduction feature, corresponding to Bi_2Te_3 deposition which can be attributed to a mutually induced co-deposition mechanism. In order to produce stoichiometric $Bi_{0.5}Sb_{1.5}Te_3$ a deposition potential in the region of −0.2 and −0.35 V vs. SCE was chosen based on these results.

Figure 2 shows a sequence of SEM images obtained from a 2 μm Ni electrode surface following potentiostatic electrodeposition at deposition potentials of −0.22 V, −0.25 V, −0.28 V, −0.31 V, −0.35 V vs. SCE respectively. The composition of the Bi-Sb-Te electrodeposits at each deposition potential was analyzed by EDX as shown in Figure 2. A small degree of surface roughness is evident in the SEM images whilst the composition of the electrodeposits was found to be stoichiometric for deposition potentials over the range −0.25 V to −0.35V vs SCE. This was then compared to results (as shown in Figure 3) in which pulsed (potentiodynamic) electrodeposition was applied to produce smoother deposits with better thermoelectric

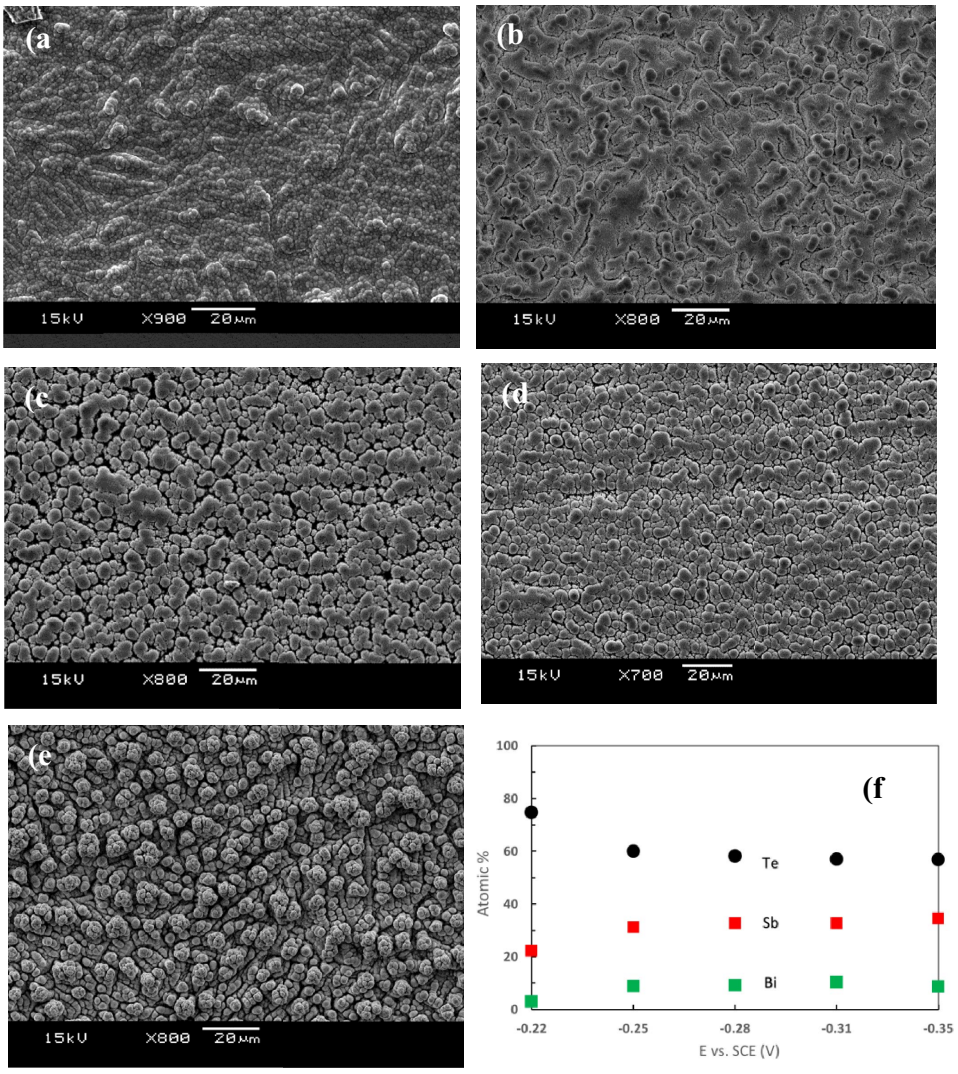

Figure 2. SEM images of 2 μm Ni film surface by potentiostatic deposition at (a) −0.22 V, (b) −0.25 V, (c) −0.28 V, (d) −0.31 V, (e) −0.35 V vs SCE, and (f) corresponding composition analyzed by EDX.

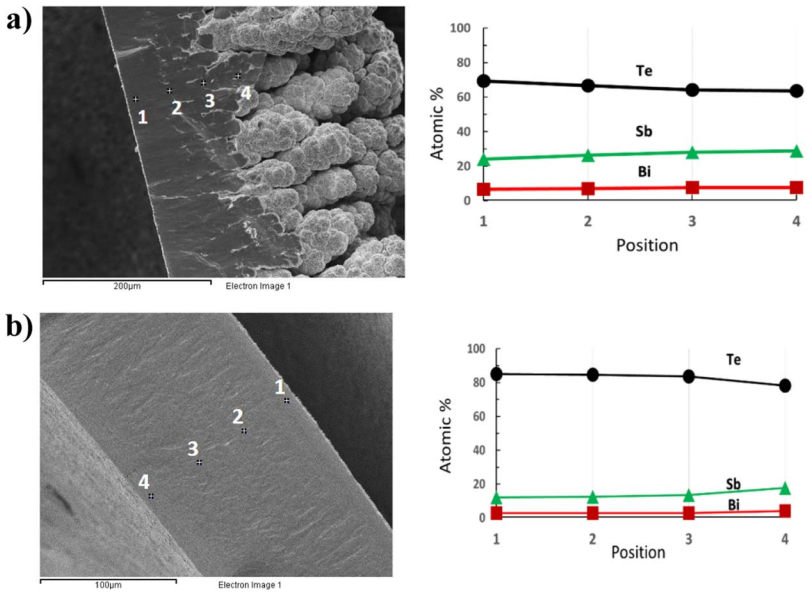

Figure 3. Cross-sectional SEM images and corresponding compositional analysis by EDX. The BiSbTe was deposited at −0.25 V (top), or −0.20 V (bottom).

properties.[16] Pulsed electrochemical deposition was then carried out by employing zero current resting pulses for 4s and deposition pulses of 10 ms at −0.2V or −0.25V vs. SCE respectively.

Figures 3a, 3b shows SEM images and EDX data of a 150 µm thick Bi-Sb-Te deposit produced by potentiodynamic electrodeposition at potentials of −0.25 and −0.20 V vs. SCE respectively. The composition across the film thickness as analyzed by EDX is also shown and reveals that at a potential of −0.25 V, the composition across the film is close to being constant and stoichiometric, whereas at a potential of −0.20 V the films are tellurium rich. As established

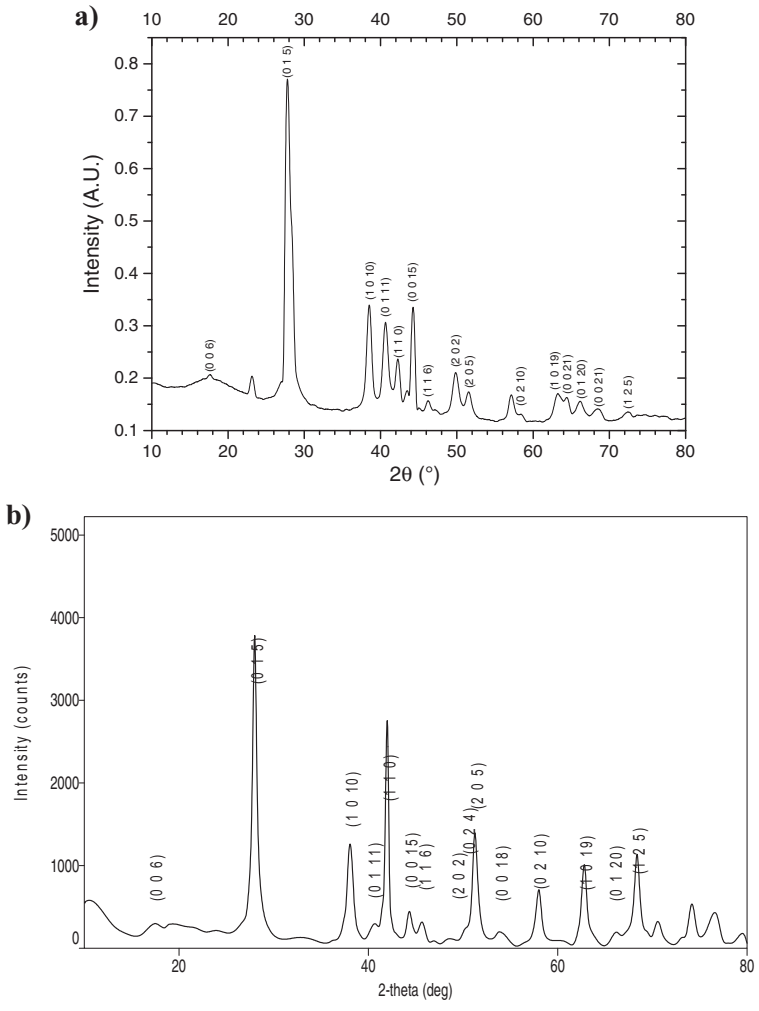

Figure 4. XRD pattern of stoichiometric $Bi_{0.5}Sb_{1.5}Te_3$ film deposited by potentiostatic electrodeposition (a) and potentiodynamic (pulsed) electrodeposition (b), obtained on a Rigaku SmartLab diffractometer using Cu-Kα radiation (λ = 1.5406 Å).

from the results presented in Figure 1 −0.20 V vs. SCE represents the lowest potential for producing stoichiometric Bi-Sb-Te deposist and the actual composition may vary which has been confirmed here by EDX anaylsis.

As the deposition progresses beyond a film thickness of 150 microns, a dendritic structure forms at a potential of −0.25 V vs. SCE which may be attributable to the depletion of the electrolyte of the respective ions.

Figure 4 shows typical XRD patterns recorded for potentiostatic (Fig. 4a) and potentiodyamic (Fig. 4b) electrodeposited $Bi_{0.5}Sb_{1.5}Te_3$ films respectively. All XRD peaks can be indexed to the rhombohedral $Bi_{0.5}Sb_{1.5}Te_3$ crystal structure according to the standard ICDD card (PDF-2/release 2012 RDB) with a space group of R3m. In both cases the (015) peak is the most prominent XRD peak, indicating that the preferred growth direction is along the (015) plane, which is in line with results in the literature.[11,12] The average grain size of the films is calculated to be 17.0 nm based on the Scherrer equation.

Hall effect measurements of the Bi-Sb-Te films resulted in p-type semiconducting behavior with a Hall mobility of up to ∼200 $cm^2/(V \cdot s)$, carrier concentration of 2.0×10^{20} cm^{-3}, electrical conductivity up to ∼100 Scm^{-1} whilst measurement of the Seebeck coefficient yielded values +150 μV/K which results in a high power factor of 2.3×10^{-4} W m^{-1} K^{-2} in case of the potentiodynamic electrodeposited bismuth antinmoy films. This is the highest power factor reported in the literature[17] to-date for electrodeposited $Bi_{0.5}Sb_{1.5}Te_3$. Transport property measurements for potentiostatically electrodeposited Bi-Sb-Te films yielded Hall mobilities of up to 90 $cm^2/(V \cdot s)$, a carrier concentration of 1.30×10^{19} cm^{-3}, electrical conductivity up to ∼86 Scm^{-1} whilst Seebeck measurements resulted in a Seebeck coefficient of +112 μV/K resulting in a power factor of 1.1×10^{-4} W m^{-1} K^{-2}.

Conclusions

Stoichiometric and uniform p-type $Bi_{0.5}Sb_{1.5}Te_3$ films with thicknesses of up to 150 μm were electrodeposited onto Ni by potentiodynamic electrodeposition at high growth rates of up to 40 μm/hour. These yielded a high power factor of 2.3×10^{-4} W m^{-1} K^{-2} and were found to exhibit better thermoelectric properties than potentiostatically deposited $Bi_{0.5}Sb_{1.5}Te_3$ films. This makes them promising materials for the fabrication of p-type legs in commercial TE devices.

Acknowledgments

We are grateful to Innovate UK for the award of a TSB grant (TS/L008157/1) and to European Thermodynamics and Scionix for their support throughout this project. The authors acknowledge the financial support of equipment grant (EP/K00509X/1) for the SmartLab. We are also grateful to Dr. Mark Light for his support with the acquisition of some of the XRD data.

References

1. L. E. Bell, *Science*, **321**, 1457 (2008).
2. D. M. Rowe, Ed. in *CRC Handbook of Thermoelectric*; CRC Press: New York, 1995
3. H. Julian Goldsmid, *Materials*, **7**, 2577 (2014).
4. P. Pichanusakorn and P. Bandaru, *Mater. Sci. Eng.*, **R67**, 19 (2010).
5. T. M. Tritt, *Science*, **283**, 804 (1999).
6. M. S. Martin-Gonzalez, A. L. Prieto, R. Gronsky, T. Sands, and A. M. Stacy, *J. Electrochem. Soc.*, **149**, C546 (2002).
7. Y. Miyazaki and T. Kajitani, *J. Cryst. Growth*, **229**, 542 (2001).
8. S. Li, M. S. Toprak, H. M. A. Soliman, J. Zhou, M. Muhammed, D. Platzek, and E. Muller, *Chem. Mater.*, **18**, 3627 (2006).
9. S.-K. Lim, M.-Y. Kim, and T.-S Oh, *Thin Solid Films*, **517**, 4199 (2009).
10. J. Kuleshova, E. Koukharenko, X. Li, N. Frety, I. S. Nandhakumar, J. Tudor, S. P. Beeby, and N. M. White, *Langmuir*, **26**, 16980 (2010).
11. F. Li W. Wang *Appl. Surf. Sci.*, **255**, 4225 (2009).
12. K. Tittes and W. Plieth, *J Solid State Electrochem*, **11**, 155 (2007).
13. W. Glatz, S. Muntwyler, and C. Hierold, *Sensors and Actuators A-Physical*, **132**, 337 (2006).
14. W. Glatz, E. Schwyter, L. Durrer, and C. Hierold, *J. Microelectrom. Sys.*, **18**, 763 (2009).
15. T. C. Monson, M. T. Lloyd, D. C. Olson, Y. J. Lee, and J. W. P. Hsu, *Adv. Mater.*, **20**, 4755 (2008).
16. C. Schumacher, K. G. Reinsberg, L. Akinsinde, S. Zastrow, S. Heiderich, W. Toellner, G. Rampelberg, C. Detavernier, J. A. C. Broekaert, K. Nielsch, and J. Bachmann, *Adv. Energy Mater.*, **2**, 345 (2012).
17. C. Boulanger, *J. Electron. Mater.*, **39**, 1818 (2010).